Macromolecules

ARTICLE

pubs.acs.org/Macromolecules

Quantitative Comparison of the Mesitoyl vs the Benzoyl Fragment in Photoinitiation: A Question of Origin

Dominik Voll,[†] Thomas Junkers,[‡] and Christopher Barner-Kowollik*[,†]

[†]Preparative Macromolecular Chemistry, Institut für Technische Chemie und Polymerchemie, Karlsruhe Institute of Technology (KIT), Engesserstr. 18, 76128 Karlsruhe, Germany

[‡]Institute for Materials Research (IMO), Polymer Reaction Design Group, Universiteit Hasselt, Agoralaan, Gebouw D, BE-3590 Diepenbeek, Belgium

Supporting Information

ABSTRACT:

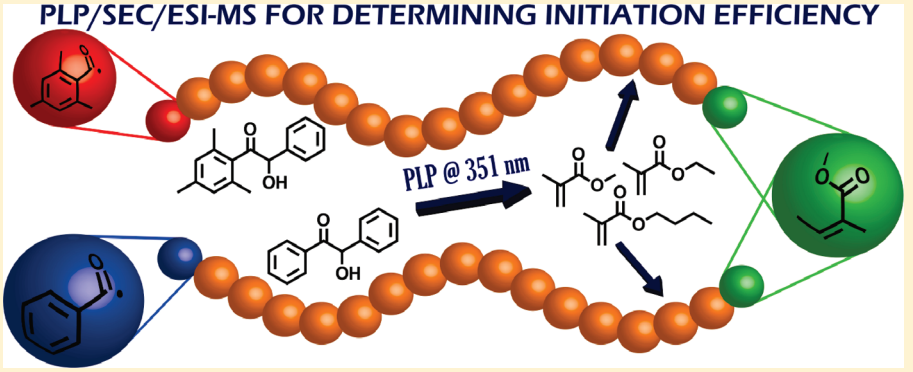

Photolytically generated radicals (at a wavelength of 351 nm) derived from the acetophenone-type photoinitiators benzoin (2-hydroxy-1,2-diphenylethanone) and 2,4,6-trimethylbenzoin (2-hydroxy-1-mesityl-2-phenylethanone, TMB) (specifically the benzoyl and mesitoyl radical) are quantified in their ability to serve as initiating species in methyl methacrylate (MMA), ethyl methacrylate (EMA), and butyl methacrylate (BMA) bulk free radical polymerizations under optimized conditions. Herein, 2,4,6-trimethylbenzoin is employed for the first time as photoinitiator in pulsed laser polymerizations (PLP) employing a high-frequency excimer laser, constituting a new source for mesitoyl radicals. The current work presents an improved method for quantifying radical efficiency of photoinitiation processes using coupled online size exclusion chromatography−electrospray ionization mass spectrometry (SEC/ESI-MS) to analyze the obtained polymers. Because of the occurrence of side reactions during the benzoin-initiated MMA polymerization, reduced laser energies (∼0.35 mJ/pulse) as well as low polymerization temperatures (∼−5 °C) were employed, which avoids side product formation. A plot of the ratio of benzoyl to mesitoyl (derived from 2,4,6-trimethylbenzoin) end groups vs the ratio of both initiators in the reaction mixture indicates that the benzoin-derived benzoyl radical is 3.0 (2.6, 2.4) times more likely to initiate the polymerization process of MMA (EMA, BMA) than the TMB-derived mesitoyl fragment. This observation is in sharp contrast to the case when mesitil is employed as a source of mesitoyl radicals (8.6 times higher likelihood of benzoyl incorporation). These results clearly support the notion that the origin of a radical species significantly determines its propensity to be incorporated at a polymer chain's terminus. The cause of such an origin dependence is tentatively assigned—at least in part—to different triplet lifetimes or intersystem crossing efficiencies (Φ_{ISC}) or both of TMB and mesitil.

INTRODUCTION

Photoinitiators are used for the polymerization of functional monomers for the generation of variable oligomers and polymers.[1] They are employed in industrial applications including the UV-curing of coatings and inks as well as for more specialized applications, such as dental restorative materials,[2,3] biomaterials,[4,5] and the fabrication of 3-dimensional objects.[6] Photoinitiation is usually applied to commence a chain growth process where both the initiating species and the growing chain ends are radicals,[7] cations,[8] or—in some cases—anions or weak bases.[9] Photoinitiators for radical polymerizations are classified as cleavage (type I, for example benzoin and derivatives) and H-abstraction type (type II, for example thioxanthone and derivatives) initiators.[10−12] The majority of type I photoinitiators

Received: January 28, 2011
Revised: March 13, 2011
Published: March 30, 2011

Scheme 1. Photolytic Decomposition Pattern of 2,4,6-Trimethylbenzoin (A), Benzoin (B), and Mesitil (C)[a]

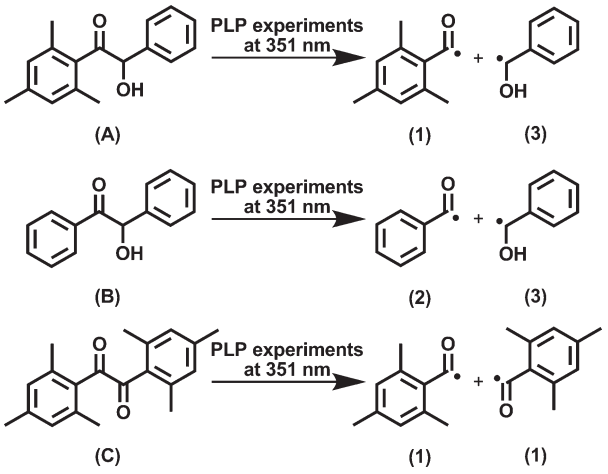

[a] The photoinitiators **A** and **B** are used in the current study for quantifying the initiation efficiency of the radical fragments (**1**, mesitoyl) and (**2**, benzoyl). To compare the latest results with our former study between **B** and **C**, the decomposition pattern of **C** is also depicted. Note that the combination of compound **C** with **B** was the subject of a previous study.[31]

are aromatic carbonyl compounds with appropriate substitution. Upon absorption of light, benzoin and its derivatives spontaneously undergo α-cleavage and generate free radicals. Benzoin and its derivatives are the most widely used photoinitiators for free radical polymerization due to their high quantum efficiency and reactivity of the generated radical fragments. Photoinitiation processes via type II photoinitiators are based on the reaction of their triplet excited states with a hydrogen donor, thereby producing an initiating radical.[12] For further details about photoinitiated polymerizations and their opportunities, the reader is referred to a recently published review by Yagci and colleagues.[13] Furthermore, photoinitiators are used in academia for pulsed laser polymerization. Pulsed laser polymerization coupled to size-exclusion chromatography (PLP-SEC), pioneered by Olaj and co-workers in 1987,[14] is the most prominent and accurate technique for the determination of the rate coefficient of propargation, k_p, today.[15−20] In a further refinement of the technique, a recent study showed that PLP in conjunction with online size exclusion chromatography—electrospray ionization mass spectrometry (SEC/ESI-MS) can successfully be applied for the determination of highly accurate propagation rate coefficients in free radical polymerization.[21] The potential of SEC/ESI-MS has been discussed in several publications.[22−24] For the PLP technique, the photoinitiators employed must be able to initiate the polymerization of a wide range of monomers, and the pathways of initiation are important to know.[25−27] Qualitative studies on photoinitiation processes have been carried out in several publications using electrospray ionization mass spectrometry (ESI-MS).[28−30] While qualitative investigations can reveal some important trends, it is of great importance to quantify the initiation ability of the different initiator fragments toward variable classes of monomers. The initiator fragments are located at the α-end groups (and if combination modes prevail also the ω-end groups) of the polymeric material and should therefore be predestinated for (quantitative) mass spectrometric analysis. In a previous investigation employing ESI-MS to quantitatively study photoinitiation processes, we have mapped in great detail the reaction products of two specific photolytically generated radical fragments during the bulk free radical polymerization of methyl methacrylate (MMA), namely the mesitoyl and the benzoyl fragments (see Scheme 1 for the structures).[31] A large disparity in net-initiation efficiency between both fragments with respect to their ability to start chain growth was found. The initiator fragments in the previous study were generated from the photoinitiators benzoin and mesitil. The observed difference in efficiency can be assigned to three effects, i.e., the actual initiation rate and/or the overall quantum yield and/or the ability of the molecule to absorb light. All three combined result in the above-noted *net-initiation* efficiency that can be compared between different photoinitiator systems. Thus, even though the rate of initiation of a certain radical fragment toward the same monomer should be universal, one may anticipate an origin dependence of the net-initiation efficiency, and it is therefore mandatory to study different sources of such fragments with respect to their abundance in the polymeric product. In here, we employ the above-mentioned PLP/SEC/ESI-MS method to quantitatively study the reaction behavior of a related couple of initiators, bearing the same initiator fragments as in our previous investigation (i.e., mesitoyl and benzoyl),[31] yet originating from different source molecules. PLPs were performed at low laser energy on a homologous series of alkyl methacrylates, differing in chain lengths of the ester side group (i.e., methyl (methyl methacrylate, MMA); ethyl (ethyl methacrylate, EMA), and butyl (butyl methacrylate, BMA)). Methacrylates are purposefully chosen as they predominantly terminate via disproportionation, providing certainty that the terminal group in the chain has truly initiated the macromolecular growth process.

The reason for employing online SEC/ESI-MS for quantifying photolytically generated radicals in their ability to serve as initiating species in the free radical bulk polymerization of variable methacrylates is due to the fact that ESI-MS spectra, which are measured via direct infusion of the polymer samples can—under certain circumstances—be less accurate (for details see the Results and Discussion section). Compared to our previous study,[31] the laser energy as well the temperature has been reduced to minimize side product formation during the free radical polymerization using the PLP technique and benzoin (**B**) as initiator. The below-described observation of unassigned signals in the ESI-MS spectra of macromolecules initiated by benzoin presented herein, may be associated with the improvement in the employed ESI-MS system in the current study (for details see the Experimental section), which is up to 10 times more sensitive compared to the ESI-MS system previously employed.[31] For quantitative evaluation of the SEC/ESI-MS spectra it is of primary importance to assign or—better eliminate—all of the side products, as long as their formation process remains unresolved. In the present study, two benzoin-type photoinitiators, i.e., benzoin (**B**) and 2,4,6-trimethylbenzoin (**A**), were employed to study the (net) efficiency of the benzoyl fragment (**2**) to initiate the free radical bulk polymerization of methyl methacrylate (MMA), ethyl methacrylate (EMA), and butyl methacrylate (BMA), which is quantitatively compared to the initiation efficiency of the mesitoyl fragment (**1**).[32]

Scheme 1 depicts the chemical structure as well as the UV-light-induced radical decomposition products of all the (in our quantitative studies) applied photoinitiators, which have been used to initiate macromolecular growth via PLP. Note that the

disproportionation product having radical fragment **3** as an end group is not the subject of the present study (for details see below). The choice for studying the comparative efficiency of benzoyl vs mesitoyl is driven by previous quantitative findings that the mesitoyl fragment—when derived from mesitil—has an 8.6 times reduced propensity to be found as a polymer end group in poly(methyl methacrylate) (pMMA) than that of the benzoyl fragment (derived from benzoin).[31] In the current study 2,4,6-trimethylbenzoin was used for the first time in photoinitiation processes of free radical bulk polymerizations of methacrylates. The reason for employing 2,4,6-trimethylbenzoin instead of mesitil is twofold: First—and most importantly—this initiator has the same general structure as benzoin (benzoin-type photoinitiator), thus potentially featuring a similar triplet lifetime and intersystem crossing (ISC) behavior, therefore allowing a differentiation of the origin of the sluggish incorporation of mesitoyl radicals when they are derived from mesitil.[27] We note that the hypothesis of similar triplet lifetimes and ISC behavior for the two initiators may not be tenable under all circumstances, as the additional methyl groups on the phenyl ring in TMB may alter the geometry of the molecule (out-of-plane twisted configurations may be preferred), leading to an altered behavior (see ref 33 for some computational evidence for such an effect). Second, the initiator comprises only one mesitoyl fragment. Therefore, the ratio of both radical fragments (coming from TMB and benzoin, respectively) as they are generated is 1:1. The primary aim of the current study is thus to quantify the net-efficiency difference (i.e., their respective propensity to be found as the initiating group at the chain end) between the benzoyl and the mesitoyl fragments, derived from benzoin and 2,4,6-trimethylbenzoin, to establish whether the propensity of the mesitoyl fragment to be found as an initiating species is a function of its origin. The following experimental strategy is employed: Mixtures of benzoin and 2,4,6-trimethylbenzoin (ranging from equimolar composition to a large excess of **A**) are prepared and subjected to pulsed laser polymerization as described in the Experimental section. The generated polymer is isolated and subjected to online SEC/ESI-MS. From the mass spectral evaluation procedure, the ratio of benzoyl and mesitoyl radicals that have initiated macromolecular growth is plotted as a function of the ratio of both initiators in the reaction mixture. The evaluation procedure for such a plot, as well as the mass spectral evaluation, is described elsewhere.[34,35] Scheme 2 depicts the expected disproportionation and combination products, which are formed in the presence of MMA as monomer (for schemes of EMA and BMA as monomer see Scheme S1 and Scheme S2). Table 1 contains the corresponding experimentally observed as well as the theoretically expected masses for the identified disproportionation and combination products in one repeat unit.

EXPERIMENTAL SECTION

Materials. Methyl methacrylate (MMA, Sigma-Aldrich, 99%, stabilized), ethyl methacrylate (EMA, Acros, 99%, stabilized), and butyl methacrylate (BMA, Acros, 99%, stabilized) were freed from inhibitor by passing through a column of activated basic alumina (Merck). Benzoin (Sigma-Aldrich, 98%) was recrystallized twice in ethanol prior to use. Benzene (Sigma-Aldrich, purris. p.a.) was dried over molecular sieves (4 Å) for 4 h. Dioxane (Acros), selenium dioxide (Acros, 99.8%), aluminum chloride (ABCR, anhydrous), and 2,4,6-trimethylacetophenone (Sigma-Aldrich, purum) were used as received. For SEC/ESI-MS measurements sodium iodide (Fluka, purris. p.a.), tetrahydrofuran (THF, Scharlau, multisolvent GPC grade, 250 ppm BHT) and methanol (VWR, chromanorm) were also employed as received. For UV/Vis measurements methanol (VWR, chromanorm) was used.

Synthesis of Mesitylglyoxal. The following preparation procedure of mesitylglyoxal is adapted from the literature.[36−38] A solution of 6.48 g of selenium dioxide (58.4 mmol, 1.00 eq), 5.00 mL of water, and 9.56 g of 2,4,6-trimethylacetophenone (9.80 mL, 58.9 mmol, 1.00 eq) in 65.0 mL of dioxane was refluxed for 5 h at 105 °C under vigorous stirring. During the heating of the solution a gradual precipitation of selenium takes place, and the color changes from colorless to yellow. The solution was decanted from the free selenium, and the dioxane was evaporated. The crude yellow product was purified via vacuum distillation. The product was collected at T = 62 °C and $p = 4.1 \times 10^{-1}$ bar as a clear yellow oil which crystallized upon cooling (yield: 2.95 g, 16.7 mmol, 28%). ESI-MS: $[M + Na]_{exp}$ = 199.1 Da and $[M + Na]_{calc}$ = 199.07 Da. ^{1}H NMR (400 MHz, $CDCl_3$) [δ, ppm]: 9.53 (s, 1H, −CHO), 6.89 (s, 2H, $-H_{arom}$), 2.31 (s, 3H, $-CH_3$), 2.18 (s, 6H, 2 × $-CH_3$). ^{13}C NMR (100 MHz, $CDCl_3$) [δ, ppm]: 196.79 (C_1), 188.30 (C_2), 141.37 (C_3), 136.47 (C_4), 131.18 (C_5), 129.09 (C_6), 21.28 (C_7), 20.16 (C_8). (For more details, see Figures S1 and S2 in the Supporting Information.)

Synthesis of 2-Hydroxy-1-mesityl-2-phenylethanone (2,4,6-Trimethylbenzoin, A). To a suspension of 1.53 g of anhydrous aluminum chloride (11.5 mmol, 2.01 eq) in 5.80 mL of benzene at 10 °C, 1.01 g of mesitylglyoxal (5.74 mmol, 1.00 eq) dissolved in 5.80 mL of benzene was added. The reaction was then vigorously stirred over a period of 2 h at 10 °C (cooled with ice). Stirring was continued overnight at ambient temperature. The reaction mixture was subsequently poured onto ice and concentrated hydrochloric acid. The organic layer was removed, and the aqueous layer was extracted twice with a minimal amount of benzene. The combined organic layers were dried over $MgSO_4$, and benzene was evaporated under reduced pressure. The crude, pale, yellowish solid was recrystallized from ethanol to give 2,4,6-trimethylbenzoin (**A**) as a white powder (yield: 0.58 g, 2.28 mmol, 40%). ESI-MS: $[M + Na]_{exp}$ = 277.2 Da and $[M + Na]_{calc}$ = 277.12 Da. ^{1}H NMR (400 MHz, $CDCl_3$) [δ, ppm]: 7.25−7.19 (m, 3H, $-H_{ph}$), 7.15−7.08 (m, 2H, $-H_{ph}$), 6.74 (s, 2H, $-H_{arom}$), 5.59 (d, ^3J = 5.2 Hz, 1H, $-H_{tert}$), 4.50 (d, ^3J = 5.5 Hz, 1H, −OH), 2.26 (s, 3H, $-CH_3$), 1.82 (s, 6H, 2 × $-CH_3$). ^{13}C NMR (100 MHz, $CDCl_3$) [δ, ppm]: 208.21 (C_1), 139.55 (C_2), 136.58 (C_3), 134.59 (C_4), 134.12 (C_5), 128.37 (C_6), 128.31 (C_7), 126.77 (C_8), 80.54 (C_9), 21.11 (C_{10}), 18.90 (C_{11}). (For more details see Figures S1 and S2 in the Supporting Information.)

Polymerizations. All MMA, EMA, and BMA samples consisted of monomer (sample volume ∼0.5 mL) with a mixture of both photoinitiators with an overall concentration of $c_{PI} = 5 \times 10^{-3}$ mol L^{-1}. The samples were carefully freed from oxygen prior to laser irradiation by purging the reaction mixture with high-purity nitrogen for 2 min. The sample vial was subsequently placed into a sample holder, which was held at a constant temperature of −5 °C by a thermostat (model: 1196D, VWR, Darmstadt, Germany). The temperature was independently measured at the sample holder. The sample temperature was allowed to equilibrate for 5 min before starting the polymerization. Photoinitiation was achieved by an excimer laser system (Coherent Xantos XS-500, XeF, frequency variable from 1 to 500 Hz, operating at a wavelength of 351 nm (pulse width ∼20 ns) and an laser energy of 2−6 mJ) at 100 Hz for an overall polymerization time of 90 000 laser pulses (∼15 min). A self-made metal filter (fine-mesh metal grid) was implemented next to the radiation exit window to obtain a reduced laser energy of ∼0.35 mJ/pulse. The laser beam, which was adjusted to an energy of close to 0.35 mJ/pulse hitting the sample, was redirected to illuminate the vial from the bottom.

UV/Vis Spectra. UV/Vis spectra were recorded at ambient temperatures using a Varian Cary 300 Bio photospectrometer.

Scheme 2. Expected Polymeric Disproportionation and Combination Peaks in the Photochemically Initiated Bulk Free Radical Polymerization of MMA in the Presence of a Cocktail of the Benzoin and 2,4,6-Trimethylbenzoin Photoinitiators Depicted in Scheme 1[a]

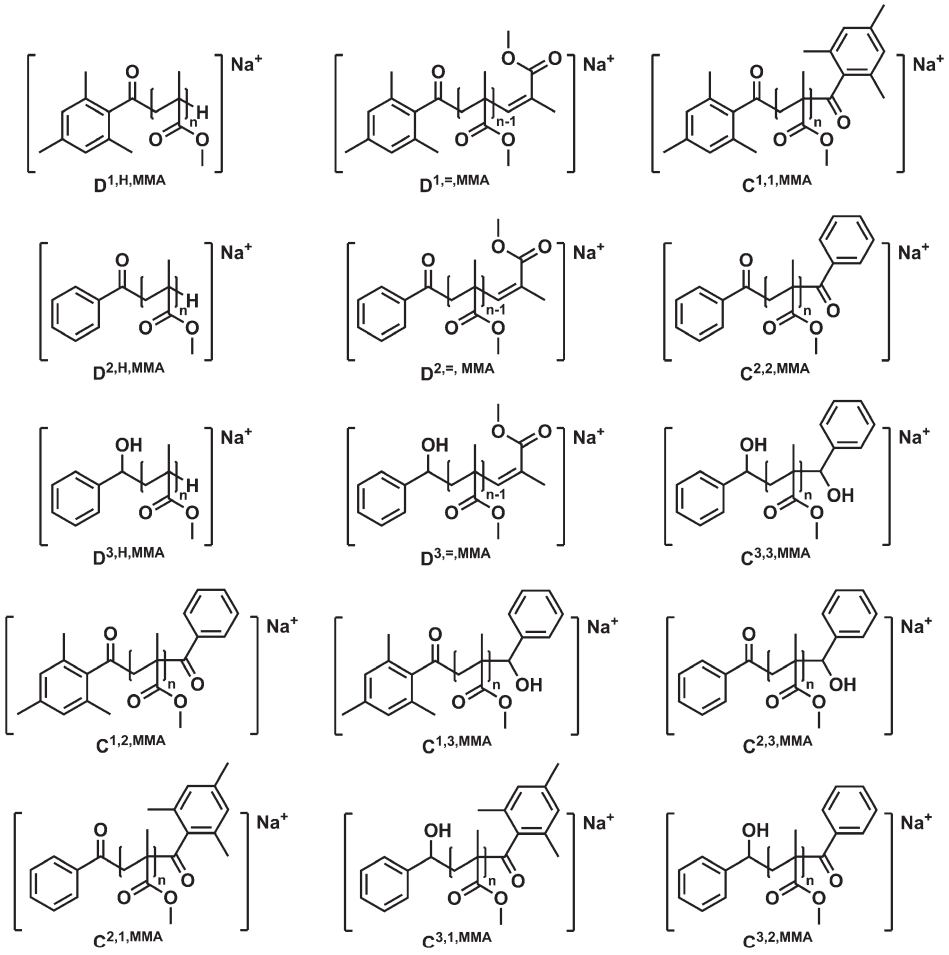

[a] Note that the position of the double bond in the unsaturated disproportionation product may also be at the site of the former α-methyl group. See Table 1 for a collation of the masses of the individual radical fragments. Furthermore, the combination products are not of interest but are mentioned because of completeness of assignment ($C^{1,2,MMA}$, $C^{2,1,MMA}$; $C^{1,3,MMA}$, $C^{3,1,MMA}$ and $C^{2,3,MMA}$, $C^{3,2,MMA}$ cannot be distinguished in the mass spectra). A detailed description of the nomenclature is given in the Results and Discussion section.

NMR. The structure of the synthesized photoinitiator was confirmed by ^{1}H-NMR spectroscopy on a Bruker AM 400 spectrometer at 400 MHz for hydrogen nuclei and 100 MHz for carbon nuclei. All samples were dissolved in $CDCl_3$.

SEC/ESI-MS. Spectra were recorded on an LXQ mass spectrometer (ThermoFisher Scientific, San Jose, CA) equipped with an atmospheric pressure ionization source operating in the nebulizer-assisted electrospray mode. The instrument was calibrated in the m/z range 195−1822 amu using a standard containing caffeine, Met-Arg-Phe-Ala acetate (MRFA), and a mixture of fluorinated phosphazenes (Ultramark 1621) (all from Aldrich). A constant spray voltage of 4.5 kV was used, and nitrogen at a dimensionless sweep gas flow rate of 2 (~3 L min^{-1}) and a dimensionless sheath gas flow rate of 12 (~1 L min^{-1}) were applied. The capillary voltage, the tube lens offset voltage, and the capillary temperature were set to 60 V, 110 V, and 275 °C, respectively. The LXQ was coupled to a Series 1200 HPLC-system (Agilent, Santa Clara, CA) consisting of a solvent degasser (G1322A), a binary pump (G1312A), and a high-performance autosampler (G1367B), followed by a thermostated column compartment (G1316A). Separation was performed on two mixed bed size exclusion chromatography columns (Polymer Laboratories, Mesopore 250 × 4.6 mm, particle diameter 3 μm) with precolumn (Mesopore 50 × 4.6 mm) operating at 30 °C. THF at a flow rate of 0.30 mL min^{-1} was used as eluent. The mass spectrometer was coupled to the column in parallel to an RI-detector (G1362A with SS420x A/D) in a setup described earlier.[23] An aliquot of 0.27 mL min^{-1} of the eluent was directed through the RI detector and 30 μL min^{-1} infused into the electrospray source after post-column addition of a 100 μM solution of sodium iodide in methanol at 20 μL min^{-1} by a microflow HPLC syringe pump (Teledyne ISCO, model 100DM). Flow rates, instrument settings, and salt concentrations were optimized to yield maximum ionization efficiency while keeping salt cluster formation to a minimum.[39] 50 μL of a polymer solution with a concentration of 5.5 mg mL^{-1} was injected onto the HPLC system.

RESULTS AND DISCUSSION

In the current work we wish to establish whether the origin of a specific photolytically generated radical (i.e., mesitoyl derived from mesitil vs mesitoyl derived from 2,4,6-trimethylbenzoin) has an influence on its ability to serve as an initiating species in free radical polymerizations. In our previous study,[31] the

dx.doi.org/10.1021/ma2001977 |Macromolecules 2011, 44, 2542–2551

Table 1. Collation of the Polymeric Product Signals Observed during SEC/ESI-MS of Poly(methyl methacrylate) Samples Generated during the Pulsed Laser-Initiated Bulk Free Radical Polymerization of MMA at 100 Hz and −5 °C[a]

species	ionization	$(m/z)^{theo}$/Da	$(m/z)^{exp}$/Da	$\Delta(m/z)$
$D^{1,H,MMA}$	Na^+	1171.6 ($n = 10$)	1171.7	0.1
$D^{l,=,MMA}$	Na^+	1169.6 ($n = 10$)	1169.7	0.1
$D^{2,H,MMA}$	Na^+	1129.6 ($n = 10$)	1129.7	0.1
$D^{2,=,MMA}$	Na^+	1127.5 ($n = 10$)	1127.6	0.1
$D^{3,=,MMA}$	Na^+	1131.6 ($n = 10$)	1131.7	0.1
$D^{3,H,MMA}$	Na^+	1129.6 ($n = 10$)	1129.7	0.1
$C^{1,1,MMA}$	Na^+	1117.6 ($n = 8$)	1117.4	0.2
$C^{2,2,MMA}$	Na^+	1133.5 ($n = 9$)	1133.7	0.2
$C^{3,3,MMA}$	Na^+	1137.6 ($n = 9$)	1137.5	0.1
$C^{l,2,MMA}$	Na^+	1175.6 ($n = 9$)	1175.6	0
$C^{1,3,MMA}$	Na^+	1177.6 ($n = 9$)	1177.5	0.1
$C^{2,3,MMA}$	Na^+	1135.5 ($n = 9$)	1135.4	0.1

[a] The table provides experimentally observed as well as theoretically expected masses for the found disproportionation (D) and combination (C) products (consisting 8 monomer units, n is the number of repeat units). The structures corresponding to the individual peaks are depicted in Scheme 2. The tabulated values correspond to the peaks displayed in Figure 2.

Scheme 3. Synthesis of 2,4,6-Trimethylbenzoin (A); 2,4,6-Trimethylacetophenone, Mesitylglyoxal

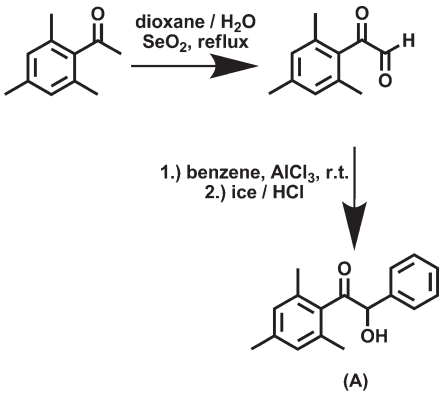

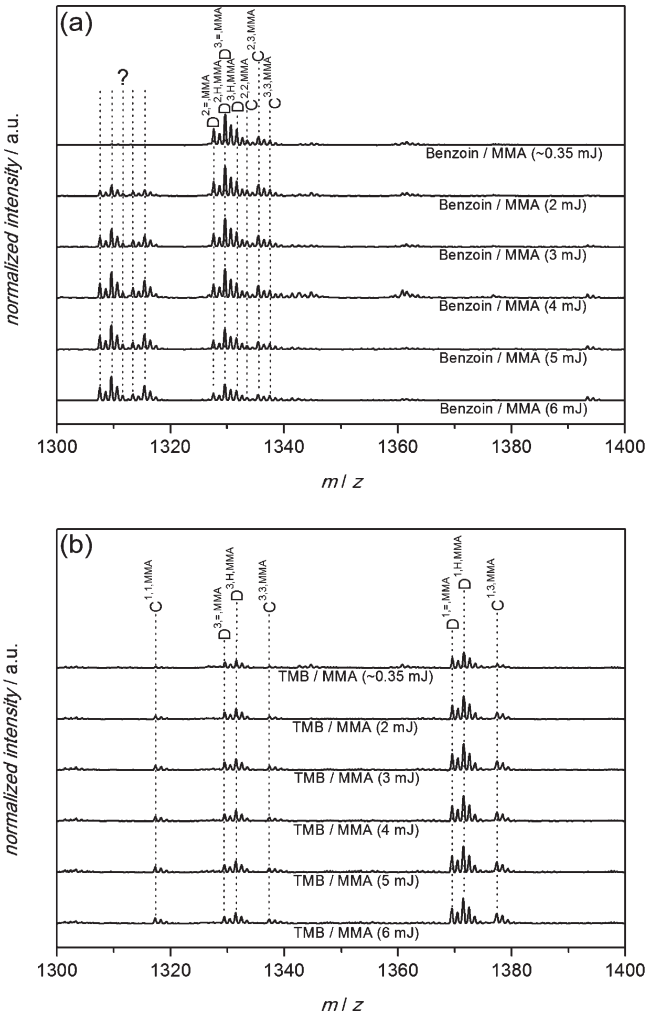

Figure 1. (a) ESI-MS spectra (one repeat unit) of benzoin-initiated pMMA obtained at variable laser pulse energies (~0.35 to 6 mJ/pulse; measured in DCM/MeOH (3:1) via direct infusion) synthesized via pulsed laser polymerization (PLP) at 100 Hz, −5 °C, and $c_{PI} = 5 \times 10^{-3}$ mol L^{-1}. (b) ESI-MS spectra (one repeat unit) of 2,4,6-trimethylbenzoin-initiated pMMA obtained at variable laser pulse energies (~0.35 to 6 mJ/pulse; measured in DCM/MeOH (3:1) via direct infusion) synthesized via pulsed laser polymerization (PLP) at 100 Hz, −5 °C, and $c_{PI} = 5 \times 10^{-3}$ mol L^{-1}. The nomenclature employed to identify the individual disproportionation and combination products is provided in Scheme 2.

effectiveness of mesitoyl (derived from mesitil) vs benzoyl (derived from benzoin) radicals for initiating MMA polymerization was established. The study concluded that it is unlikely that a potential (relative) net-efficiency difference of up to a factor of 8.6 (or potentially up to 86 when additionally considering the very different (factor of ~10) UV absorptivities of mesitil and benzoin at 351 nm, see also below) is solely caused by a difference in the intersystem crossing ability of mesitil or its triplet lifetime (or a combination of both).[31] Employing an alternative photoinitiator to mesitil, which also bears the mesitoyl fragment, should aid in solving the question of origin dependence. Such an initiator is 2,4,6-trimethylbenzoin (**A**, TMB), bearing a mesitoyl fragment (**1**) and a hydroxyl fragment (**3**) (see Scheme 1). TMB is a completely different type of initiator compared to mesitil (i.e., TMB being of the benzoin type) and should thus be ideally suited for a comparison with mesitil. Concomitantly, we are interested in quantifying the net-initiation efficiency of the benzoyl fragment (derived from benzoin) and the mesitoyl fragment (derived from 2,4,6-trimethylbenzoin) in photochemically induced PLP experiments with MMA, EMA, and BMA as monomer to assess a potential change in relative reactivity with a change in monomer. 2,4,6-Trimethylbenzoin was synthesized according to a literature procedure (see Experimental section) and is used for the first time as a photoinitiator in PLP experiments with the above-mentioned monomers. To ensure that TMB absorbs UV light at 351 nm, a UV/Vis spectrum was recorded (see Figure 5). Within the current study all assigned signals obtained in ESI mass spectra were labeled according to the following nomenclature: Disproportionation peaks occur in pairs removed by 2 amu from each other. Thus, each peak is labeled with $D^{\nu,=,x}$ or $^{\nu,H,x}$, where ν denotes the radical fragment that has initiated the polymerization ((**1**), (**2**) or (**3**),

see Scheme 1) and x denotes the monomer (MMA, EMA, or BMA). Combination products are mentioned for the sake of completeness of the assignments, yet they are of limited use in the present study as it is not possible to differentiate whether they have been generated by initiation or termination of macromolecular growth. All combination peaks are labeled with $C^{v,w,x}$ where v and w denotes the radical fragment as end group (see Scheme 1) and x denotes the monomer (MMA, EMA, or BMA).

Reducing the Laser Energy. During the work with freshly recrystallized benzoin as photoinitiator in photochemically initiated free radical bulk polymerizations of MMA, EMA, and BMA using the PLP method a surprising and unexpected observation was made. The polymeric material, synthesized via the PLP method up to 3% conversion, was analyzed with high sensitivity ESI-MS where each repeat unit of the polymer should only show four disproportionation products (in case of MMA as monomer: $D^{2,H,MMA}$, $D^{2,=,MMA}$, $D^{3,H,MMA}$, $D^{3,=,MMA}$; see Scheme 2) as well as three combination products (in case of MMA as monomer: $C^{2,2,MMA}$, $C^{3,3,MMA}$, $C^{2,3,MMA}$; see Scheme 2). Optimization of the reaction temperature (−5 °C) leads to a minimization of the combination products; thus, mainly disproportionation products were obtained in the ESI-MS spectra. However, the ESI-MS spectra in the present work show a new set of signals, which cannot be assigned to any known disproportionation or combination product (see Figure 1a, peak series denoted with a question mark). Neither can new radical fragments derived from benzoin nor salt adducts be assigned to the unexpected signals (denoted with a question mark in Figure 1a). The only successful option to eliminate the side products from the polymer was to minimize the laser energy. The employed laser system provides stable laser energies down to 2 mJ/pulse. Figure 1a depicts the ESI-MS spectra of benzoin-initiated pMMA synthesized at different laser energies via the PLP method. The energy series indicates that the side products are energy dependent (less laser energy leads to less side products); however, at the lowest stable laser energy of 2 mJ the ESI-MS spectra are not yet free of side products as evident from Figure 1a (see peak ensemble at 1307.6 m/z). Only through the subsequent installation of a fine-mesh metal grid as beam attenuator next to the beam output window was it possible to reduce the laser energy to ∼0.35 mJ/pulse. With a significant reduction in laser energy the ideally expected scenario was achieved, i.e., the disappearance of the unassigned signals. Clearly, a large energy input into benzoin opens—primary or secondary—reaction channels that lead to unexpected products. This alone is a significant observation since such fragments can have disturbing effects on PLP or any other technique relying on photoinitiation and 2 mJ/pulse is usually considered a moderate (or even low) energy input for a PLP experiment. Regardless, it has thus become feasible to obtain side product free benzoin-initiated pMMA, pEMA, and pBMA samples via a reduction of the laser energy. A photoinitiator concentration or temperature dependence of the side product formation was not detected.

To establish the behavior of the new initiator during PLP, a second set of polymerizations under variation of the incident energy was carried out for 2,4,6-trimethylbenzoin-initiated MMA polymerization. The corresponding mass spectra are depicted in Figure 1b. Pleasingly, no effect of the laser energy on the product distribution can be observed; only the four expected disproportionation products (in case of MMA as monomer: $D^{1,H,MMA}$, $D^{1,=,MMA}$, $D^{3,H,MMA}$, $D^{3,=,MMA}$; see Scheme 2) and three combination products (in case of MMA as monomer: $C^{1,1,MMA}$, $C^{3,3,MMA}$, $C^{1,3,MMA}$; see Scheme 2) are identified in the ESI-MS spectra. A collation of the polymeric product signals observed during ESI-MS via direct infusion of benzoin as well as 2,4,6-trimethylbenzoin initiated pMMA samples is shown in Table 1. For further quantification studies of these two photoinitiators the following pulsed laser polymerization conditions were used: f = 100 Hz, T = −5 °C, E ∼ 0.35 mJ/pulse and an overall concentration of the photoinitiators of c_{PI} = 5 × 10^{-3} mol L^{-1}.

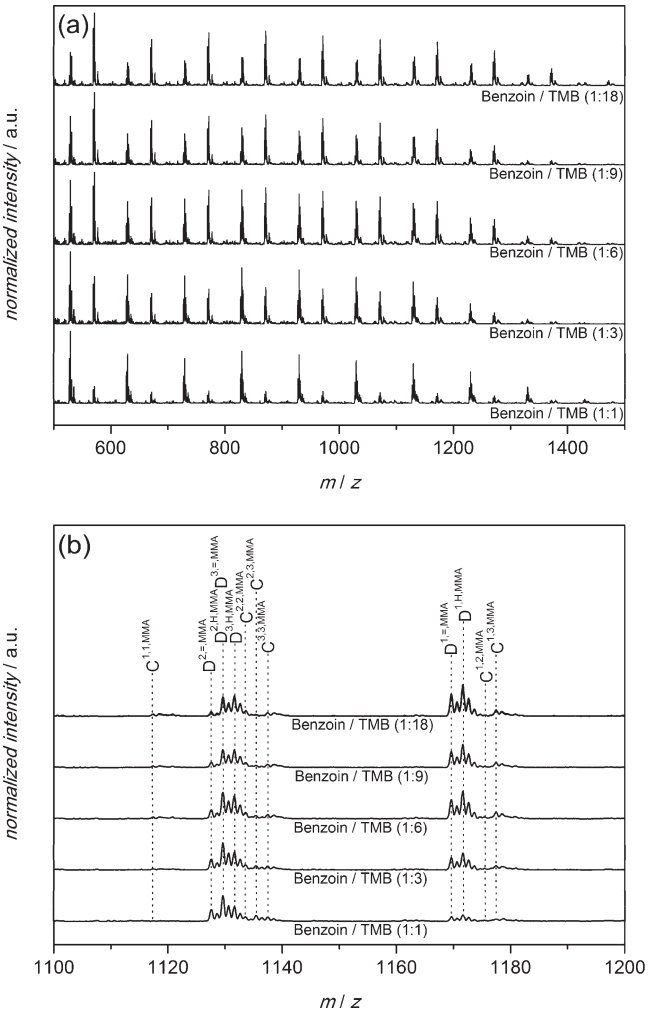

Figure 2. (a) SEC/ESI-MS overview spectra of polymeric material obtained from five different ratios of benzoin/2,4,6-trimethylbenzoin-initiated ($c_{PI,0}$ = 5 × 10^{-3} mol L^{-1}, 1:1, 1:3, 1:6, 1:9, 1:18) PLP of MMA_{bulk} at ∼0.35 mJ laser energy, 100 Hz, −5 °C. The figure depicts the singly charged products ionized with sodium iodide at a retention time between 16.86 and 19.93 min. (b) Zoom into one repeat unit of the SEC/ESI-MS overview spectra of polymeric material obtained from five different ratios of benzoin/2,4,6-trimethylbenzoin-initiated ($c_{PI,0}$ = 5 × 10^{-3} mol L^{-1}, 1:1, 1:3, 1:6, 1:9, 1:18) PLP of MMA_{bulk} at ∼0.35 mJ laser energy, 100 Hz, −5 °C. For the masses of the assigned products see Table 1. The nomenclature employed to identify the individual disproportionation and combination products is provided in Scheme 2.

Initiator Cocktails of Benzoin and 2,4,6-Trimethylbenzoin. Figure 2a provides a depiction of all SEC/ESI mass spectra recorded of pMMA, generated via the pulsed laser polymerization of MMA in the presence of different mixtures of benzoin and 2,4,6-trimethylbenzoin (1:1, 1:3, 1:6, 1:9, 1:18). Furthermore,

dx.doi.org/10.1021/ma2001977 |Macromolecules 2011, 44, 2542–2551

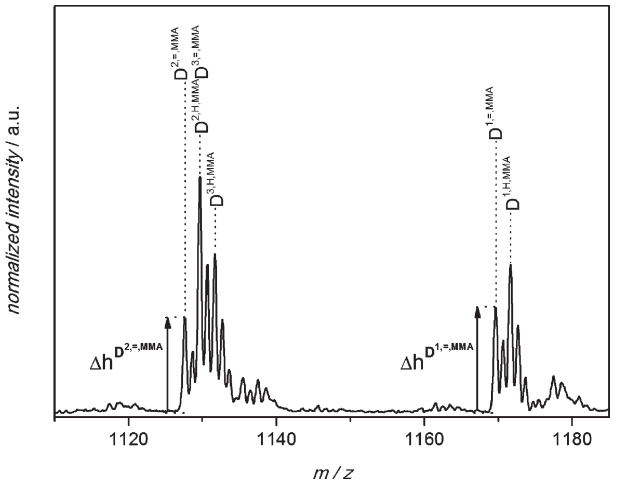

Figure 3. Enlarged section of the two disproportionation peak ensembles associated with polymer chains (pMMA) initiated by radical fragments **1**, **2**, and **3** (initiator ratio **B**:**A** = 1:3). The first signal employed for evaluation purposes is $D^{2,=,MMA}$ as it is the only isotopically nonoverlapping signal derived from benzoin. The second signal employed for quantitative evaluation purposes is $D^{1,=,MMA}$ derived from 2,4,6-trimethylbenzoin. The height of both signals in every repeat unit is employed to calculate the quantitative ratio between these two initiator fragments at the polymer chain terminus.

Figure 2b shows a representative repeat unit of the above mass spectra, with every peak labeled according to the above-noted nomenclature. The expected and found masses for the depicted representative unit are collated in Table 1. The additionally—to a much less part—occurring combination products are of no interest for deducing initiation efficiencies as explained above.

Inspection of Table 1 indicates that the theoretically and experimentally expected masses agree well within the accuracy of the mass spectrometric analysis (±0.2 Da). Such an agreement is found in every repeat unit and is representative for any initiator mixture composition employed within the current study (data for pEMA, pBMA and tables for the expected masses can be found in Figures S4 and S5 as well as Table S1 (for pEMA); Figures S7 and S8 as well as Table S2 (for pBMA) in the Supporting Information). Before proceeding to a quantitative analysis of the individual disproportionation peaks, it is worthwhile to briefly provide a qualitative description of how the SEC/ESI mass spectra changes with increasing amounts of 2,4,6-trimethylbenzoin in the initiation cocktail. For this purpose a reconsideration of Figure 2b is necessary. Inspection of this figure demonstrates that with increasing amounts of 2,4,6-trimethylbenzoin in the reaction mixture the number of chains carrying a mesitoyl end group increases ($D^{1,=,MMA}$) and the number of chains carrying a benzoyl group decreases ($D^{2,=,MMA}$). Qualitatively, one can also note that a relatively low amount of 2,4,6-trimethylbenzoin in the initiation cocktail is needed to achieve a significant signal of $D^{1,=,MMA}$. Compared to our previous study employing benzoin/mesitil mixtures,[31] a smaller amount of the mesitoyl bearing photoinitiator is necessary to achieve a significant signal. To place this qualitative observation onto a quantitative basis, the disproportionation peaks corresponding to the chains initiated with mesitoyl radicals (**1**) depicted in Figures 2b and 3 are placed into relation to the peaks associated with chains initiated by benzoyl radicals (**2**). The signals which are directly and quantitatively compared to each other need to be free of isobaric overlap with any other peaks. The disproportionation peak ensembles of all occurring radicals (**1**, **2**, and **3**) is depicted in Figure 3.

The enlarged disproportionation peak ensemble shown in Figure 3 demonstrates that only the peaks labeled with $D^{2,=,MMA}$ and $D^{1,=,MMA}$ are free of any isobaric interference. The isotopic pattern of the disproportionation products associated with $D^{1,=,MMA}$ and $D^{1,H,MMA}$ overlap with each other; for this reason, it is only possible to use $D^{1,=,MMA}$ for quantitative evaluations. In the case of the isotopic pattern associated with $D^{2,=,MMA}$, $D^{2,H,MMA}$, $D^{3,=,MMA}$, and $D^{3,H,MMA}$ the situation is more complex. Radical fragments **2** and **3** differ in molecular weight by 2 Da, leading to an unavoidable overlap of both disproportionation signals. The signals for $D^{2,H,MMA}$ and $D^{3,=,MMA}$ appear at m/z = 1129.6, making their quantitative evaluation nonfeasible. In addition, the isobaric overlap does not allow obtaining quantitative information about the initiation ability of **3**. It is also important to compare disproportionation products that carry an identical end group (unsaturated vs unsaturated or saturated vs saturated). Thus, the only choice for quantitatively evaluating the SEC/ESI mass spectra is to compare $D^{2,=,MMA}$ with $D^{1,=,MMA}$. For the other investigated polymers, (pEMA and pBMA) the same considerations apply ($D^{2,=,EMA}$ vs $D^{1,=,MMA}$ and $D^{2,=,BMA}$ vs $D^{1,=,BMA}$ (for further information see Figure S5 and Scheme S1 (for pEMA); Figure S8 and Scheme S2 (for pBMA) in the Supporting Information). Figure 3 additionally indicates how the heights $\Delta h^{D2,=,MMA}$ and $\Delta h^{D1,=,MMA}$ are defined, which are employed for the mass spectrometric evaluation procedure.

Data Analysis and Evaluation of the SEC/ESI-MS Spectra. First of all, it should be mentioned why online SEC/ESI-MS is used instead of direct infusion ESI-MS for the determination of the disproportionation signals. Direct infusion ESI mass spectra in the range of 200−2000 m/z show a slightly rising baseline, caused by the presence of multiply charged ions from higher mass ranges. Such multiply charged ions appear in the lower m/z range (up to 2000 m/z) and lead to a mild, yet constant, baseline shift. For our evaluation method of the mass spectra an accurate measure of the height of the disproportionation products (as mentioned above) is required. Therefore, it is of importance to have a constant baseline as otherwise the derived initiation efficiency of the different radicals is beset with an error. The advantage of online SEC/ESI-MS is the possibility of choosing only the singly charged ion region (defined range in the RI trace) of an entire mass spectrum. By employing SEC/ESI-MS for determining $D^{1,=,MMA}$ and $D^{2,=,MMA}$, it is, however, only possible to evaluate 8 or 9 repeat units within one mass spectrum (with ESI-MS direct infusion it is possible to evaluate in the range of up to 15 repeat units). Yet, it makes practically no difference for the final initiation ratios when 7 repeat units less are used for the evaluation of the mass spectra. In the most simple and straightforward approach for evaluating the mass data in the current work, the height of the only two peaks that do not show isobaric overlap ($D^{1,=,MMA}$ and $D^{2,=,MMA}$), $\Delta h^{Dv,=,x}$ is evaluated in each repeat unit. Figure 3 depicts a graphical representation on how $\Delta h^{Dv,=,x}$ is determined. Furthermore, the height of the individual peaks can be employed to arrive at the mole fraction of the disproportionation product $D^{1,=,MMA}$, $F(i)$ (see eq 1). Nevertheless, it is important to establish if there exists any potential chain length dependent mass bias. For this purpose we have taken a modified method from Günzler et al. established in previous quantitative mass spectrometric evaluations.[34,35] The modified approach we have taken in here is equivalent to that employed in our previous study on the mesitil/benzoin pairing.[31]

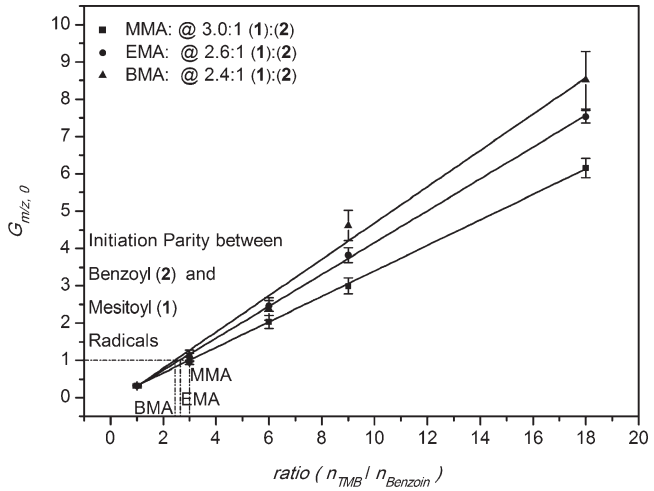

Figure 4. Plotted is the ratio of the intensities of the disproportionation products corresponding to polymer chains (pMMA, pEMA, and pBMA) initiated with a benzoyl radical (derived from benzoin) and a mesitoyl radical (derived from 2,4,6-trimethylbenzoin) vs the ratio of both initiators in the reaction mixture (ratio = n_{TMB}:$n_{benzoin}$). An evaluation procedure has been adopted, which allows for the minimization of mass bias and yields the mass bias free intensity ratio $\langle G' \rangle_{\Delta m/z,0}$. The figure also presents the initiation parity between the benzoyl and the mesitoyl radical at $\langle G' \rangle_{\Delta m/z,0} = 1$ from pMMA, pEMA, and pBMA. The calculation procedure for the error bars is given in the Supporting Information.

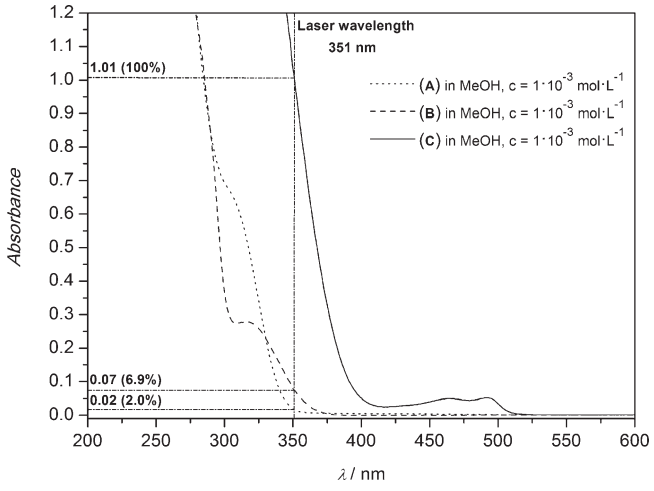

Figure 5. UV spectra of the employed photoinitiators, dissolved in MeOH at a concentration of $c_{PI} = 1 \times 10^{-3}$ mol L^{-1} to compare the absorbance at the laser wavelength of 351 nm with mesitil (**C**) (set to 100%).

$$F(i) = \frac{\Delta h^{D^{1,=,MMA}}(i)}{\Delta h^{D^{1,=,MMA}}(i) + \Delta h^{D^{2,=,MMA}}(i)} \quad (1)$$

$$G(i) = \frac{\Delta h^{D^{1,=,MMA}}(i)}{\Delta h^{D^{2,=,MMA}}(i)} \quad (2)$$

$$G'(i, i-1) = \frac{\Delta h^{D^{1,=,MMA}}(i)}{\Delta h^{D^{2,=,MMA}}(i-1)} \quad (3)$$

$$G''(i, i+1) = \frac{\Delta h^{D^{1,=,MMA}}(i)}{\Delta h^{D^{2,=,MMA}}(i+1)} \quad (4)$$

The basic equations for this approach are shown in eqs 2−4, where $G(i)$ is the ratio of the peak heights of $D^{1,=,MMA}$ and $D^{2,=,MMA}$ $\forall$ i (where i is the present repeat unit, $(i-1)$ on repeat unit lower and $(i+1)$ one repeat unit higher). After averaging, one receives $\langle G \rangle$, $\langle G' \rangle$, and $\langle G'' \rangle$, which can be plotted as $\langle G \rangle_{\Delta m/z,0}$ against the used initiator ratios, yielding a mass bias free ratio of the two disproportionation products in the polymer sample (the same procedure is used for the evaluation of the pEMA and pBMA samples).

For the mole fraction diagrams as a function of i of all monomers see Figure S3 (for pMMA), Figure S6 (for pEMA), and Figure S9 (for pBMA) in the Supporting Information. As mentioned above, they depict the mesitoyl radicals that have initiated the bulk free radical polymerization process towards the different monomers as a function of the analyzed chain length, i. Note that equal initiation ability is observed at $F(i) = 0.5$. Two important observations can be made: (i) $F(i) = F$; i.e., there is no dependence of F on the mass range that has been analyzed, implying that mass bias effects are not pronounced. (ii) Nearly 3 times excess of 2,4,6-trimethylbenzoin over benzoin is required (in the case of MMA) to achieve an identical number of chains initiated with mesitoyl and benzoyl radical fragments. In the case of EMA and BMA the situation is similar (see below).

The mass bias corrected plot of $G(i)$, $\langle G \rangle_{\Delta m/z,0}$, is used to obtain the direct ratio of chains initiated with mesitoyl fragments over those initiated with benzoyl radicals. This allows direct and quantitative comparison of the initiation efficiency of benzoin and 2,4,6-trimethylbenzoin with respect to the benzoyl and mesitoyl radicals. Inspection of Figure 4 shows a linear correlation between the ratio of benzoin to 2,4,6-trimethylbenzoin in the reaction mixture and $\langle G \rangle_{\Delta m/z,0}$ of the benzoyl and mesitoyl radicals that have initiated the polymerization process. Parity in the initiation between 2,4,6-trimethylbenzoin and benzoin derived fragments ($\langle G \rangle_{\Delta m/z,0} = 1$) occurs at an initiator mixture composition of 3.0 (MMA), 2.6 (EMA), and 2.4 (BMA). Considering the error bars given in Figure 4, one can note that there is a clear difference in the initiation parity between MMA and EMA/BMA, while the difference between pEMA and pBMA is not as pronounced.

The reason for the slight disparity between the three monomers may be caused by their different densities and viscosities as well as the mobility of the ester side chains. All these factors can have an impact on the polymerization behavior and especially on the solvent cage around the fragmenting photoinitiator, thus changing its net-efficiency. Via inspection of Figure 4, one can come to the conclusion that benzoyl radicals are a factor 3.0 (2.6, 2.4) more efficient in reacting with MMA (EMA, BMA) in the initiation of bulk free radical polymerizations than mesitoyl radicals derived from 2,4,6-trimethylbenzoin. This is a surprising quantitative experimental finding because our former study with mesitil as source for mesitoyl radicals demonstrated that benzoyl radicals are a factor 8.6 more likely in being found as a pMMA chain terminus.[31] These results support our hypothesis that not only the reactivity of specific radicals in relation to each other is an important parameter, but furthermore the origin of a specific radical plays a key role in determining its availability to initiate macromolecular growth. As noted above, upon inspection of

dx.doi.org/10.1021/ma2001977 |*Macromolecules* 2011, 44, 2542–2551

Figure 4, small differences between pMMA, pEMA and pBMA can be observed. However, the difference is small at low ratios of **B**:**A** and significantly at higher ratios of **B**:**A**.

To establish whether the observed difference in the propensity of the mesitoyl vs the benzoyl fragment to initiate the polymerization is potentially caused by a difference in the UV absorptivity, it is mandatory to establish whether the two initiators absorb UV light of 351 nm equally well. Figure 5 depicts a comparative set of UV spectra (mesitil, benzoin, and 2,4,6-trimethylbenzoin). At a concentration of $c_{PI} = 1 \times 10^{-3}$ mol L^{-1} (in methanol) and an optical path length of 10 mm, mesitil (**C**), benzoin (**B**), and 2,4,6-trimethylbenzoin (**A**) have an absorption of 1.1 (set to 100%), 0.07 (6.9%), and 0.02 (2.0%), respectively. It is important to note that mesitil features the highest absorbance, yet in PLP experiments with MMA at low laser energy (conditions: f = 100 Hz, $T = -5$ °C, $E \sim 0.35$ mJ, $c_{PI} = 5 \times 10^{-3}$ mol L^{-1}) it was not possible to obtain polymer. The cause for this observation may be twofold: First, it implies that a certain (relatively high) amount of energy (of photons featuring a 351 nm wavelength) is required—in the case of mesitil—to cause a significant decay of the photoinitiator (the generation of radicals occurs out of T_1 via intersystem crossing, ISC). The above experimental finding supports our quantitative results that the mesitoyl radical—when derived from mesitil—is found 8.6 times less as end group with respect to the benzoyl radical in pMMA. Second, in addition to the efficiency of intersystem crossing (Φ_{ISC}) the question of the lifetime of the triplet state needs to be considered. The longer the triplet lifetime, the higher the chances that deactivation processes can reduce the quantum yield for the forming radical (Φ_R). In the current system (benzoin/2,4,6-trimethylbenzoin, ~0.35 mJ/pulse) the UV absorbance of 2,4,6-trimethylbenzoin is more than 3.5 times less with respect to benzoin. Our experimental quantitative finding that the mesitoyl radical can be found ~3 times less as initiating group than the benzoyl radical in bulk free radical polymerizations of MMA, EMA, and BMA appears to directly reflect the reduced ability of TMB to absorb the laser UV light, thus potentially being the cause for the provision of less mesitoyl radicals per single laser pulse. If this notion is accepted, the conclusion may be drawn that both initiators TMB and benzoin—although having different UV absorbtivities at 351 nm—feature similar Φ_{ISC} as well as triplet lifetimes. Considering their structural similarities, such a hypothesis may not be entirely untenable. However, it must be noted that the differences in UV absorbance (at 351 nm) which correspond to the difference in the net-initiation efficiencies may be purely coincidental. Nevertheless, these observations may imply that the previously observed 8.6 times difference[31] (which rises up to a factor of 86 when considering that mesitil absorbs ~10 times more energy at 351 nm than benzoin and the (possibly questionable, see above) assumption is made that the difference in UV absorbance is directly translated into a reduced ability to provide radicals) in the net-initiation efficiency between mesitoyl and benzoyl radicals derived from mesitil and benzoin is potentially caused by a significantly increased triplet lifetime of mesitil (leading to more deactivation processes), a strongly reduced Φ_{ISC} (leading to a smaller population of T_1), or a combination of both. Irrespective of the individual contributions of the factors governing the net-efficiency, the present data unambiguously evidence a strong origin dependence of the propensity of photolytically generated radical fragments for initiating polymerizations. In principle, a direct comparison of the mesitoyl and the benzoyl fragment could be made if an initiator is employed that produces both fragments at the same time. From such an initiator, i.e., 2,4,6-trimethylphenylbenzil (1-mesityl-2-phenylethane-1,2-dione), interferences from energy transitions or cage effects on the initiation process can be excluded. Thus, such an initiator was consequently synthesized[40] and subjected to PLP as well as the above product evaluation procedure. Unfortunately, when initiated with low-energy laser pulses (~0.35 mJ/pulse), no polymer was produced as was already observed with mesitil (see the discussion above). At higher incident laser energies (6 mJ/pulse), significant side products were observed making a reliable evaluation of the disproportionation peaks impossible.

Absolute rate coefficients for the addition of benzoyl and mesitoyl radicals to *n*-butyl acrylate have been previously reported using laser flash photolysis and fast time-resolved infrared spectroscopy (TR-IR).[41] Although the current study investigates methacrylates, a comparison with the data reported in the above study may nevertheless be instructive. The rate coefficients for the addition to *n*-butyl acrylate read $k = 2.7 \times 10^5$ M^{-1} s^{-1} for the benzoyl radical (derived from 1-hydroxycyclohexyl phenyl ketone) and $k = 1.8 \times 10^5$ M^{-1} s^{-1} for the mesitoyl radical (derived from (2,4,6-trimethylbenzoyl)diphenylphosphine oxide). The rate coefficient for the addition of the benzoyl radical to *n*-butyl acrylate is thus 1.5 times higher than that of the mesitoyl radical, thus indeed suggesting a somewhat decreased reactivity of the mesitoyl radical. If one entertains the possibility that a similarly (small) difference in reactivity holds for the two radicals toward addition to methacrylate monomers, the conclusion can be drawn that the difference in net-initiation efficiency found between mesitoyl and benzoyl (a factor of 8.6 when the mesitoyl radical is derived from mesitil[31] and a factor of close to 3.0 when the mesitoyl radical is derived from TMB) is not, however, primarily due to a difference in their reactivity toward the monomer, but rather caused by variable triplet lifetimes and ISC efficiencies (as well as potential cage effects). However, at this stage no definite conclusion is possible, as this would require detailed knowledge of the above parameters. Regarding the question of the generally increased relative termination ability of the mesitoyl radical (compared to the benzoyl radical) as suggested earlier from qualitative data based on both radicals being derived from benzoin and bis(2,4,6-trimethylbenzoyl)phenylphosphine oxide,[29] caution needs to be exercised: Origin effects may also play a significant role in governing the relative propensity of primary radicals to undergo termination and initiation reactions.

CONCLUSIONS

Within the current contribution we present an improved method for determining initiator efficiencies in the system of benzoin and 2,4,6-trimethylbenzoin toward MMA, EMA, and BMA, via online SEC/ESI-MS, which enables collection of baseline-shift free mass spectra for the precision evaluation of photolytically generated end groups in macromolecules. In addition, reducing the temperature to −5 °C to further reduce combination products and reducing the laser energy by employing a beam attenuator leads to the formation of side product free polymers that only carry the characteristic benzoin-type fragments as end groups. In addition, 2,4,6-trimethylbenzoin was employed for the first time as a photoinitiator in the bulk free radical polymerization using the PLP method. The key finding of the current study is that the benzoyl radical (derived from benzoin) is 3.0 times more likely to initiate the polymerization

process of MMA than the mesitoyl radical (derived from 2,4,6-trimethylbenzoin) (2.6 (EMA) and 2.4 (BMA)). These data—in comparison with previously recorded initiation efficiency data of mesitoyl and benzoyl fragments derived from mesitil and benzoin—provide strong evidence that a significant origin dependence of the initiators' net-efficiency to commence macromolecular growth. Further studies in our laboratories will focus on directly measuring the triplet lifetimes of mesitil and TMB as well as establishing whether radical cage effects can contribute to differences in initiation ability.

■ ASSOCIATED CONTENT

Ⓢ Supporting Information. NMR data, mole fraction plots for all polymers, SEC/ESI-MS mass spectra of pEMA and pBMA, tabulation of the observed signals in SEC/ESI-MS spectra, and structural assignments for pEMA and pBMA as well as an assessment of errors. This material is available free of charge via the Internet at http://pubs.acs.org.

■ AUTHOR INFORMATION

Corresponding Author

*Tel (+49) 721 608-45642; Fax (+49) 721 608-45740; e-mail christopher.barner-kowollik@kit.edu.

■ ACKNOWLEDGMENT

C.B.-K. acknowledges financial support for the current project from the German Research Council (DFG) as well as from the Karlsruhe Institute of Technology (KIT) in the context of the Excellence Initiative for leading German universities and the Ministry for Science and Arts of the state of Baden-Württemberg. We thank Prof. P. Vana from the University of Göttingen for the initial provision of the beam attenuators.

■ REFERENCES

(1) Kaur, M.; Srivastava, A. K. *J. Macromol. Sci., Part C: Polym. Rev.* **2002**, *42*, 481–512.
(2) Ge, J.; Trujillo, M.; Stansbury, J. W. *J. Dent. Matter* **2005**, *21*, 1163–1169.
(3) Anseth, K. S.; Newman, S. M.; Bowman, C. N. *Adv. Polym. Sci.* **1995**, *122*, 177–217.
(4) Fisher, J. P.; Dean, D.; Engel, P. S.; Mikos, A. G. *Annu. Rev. Mater. Res.* **2001**, *31*, 171–181.
(5) Anseth, K. S.; Metters, A. T.; Bryant, S. J.; Martens, P. J.; Elisseeff, J. H.; Bowman, C. N. *J. Controlled Release* **2002**, *78*, 199–209.
(6) Sun, H. B.; Kawata, S. *Adv. Polym. Sci.* **2004**, *170*, 169–273.
(7) Arsu, N.; Reetz, I.; Yagci, Y.; Mishra, M. K. *Photoinitiated Radical Vinyl Polymerization*. In *Handbook of Vinyl Polymers: Radical Polymerization, Process, and Technology*; Mishra, M. K., Yagci, Y., Eds.; CRC Press: Boca Raton, FL, 2009; Vol. 20, pp 141−204.
(8) Yagci, Y.; Reetz, I. *Prog. Polym. Sci.* **1998**, *23*, 1485–1538.
(9) Kutal, C.; Grutsch, P. A.; Yang, D. B. *Macromolecules* **1991**, *24*, 6872–6873.
(10) Gruber, H. F. *Prog. Polym. Sci.* **1992**, *17*, 953–1044.
(11) Hageman, H. *J. Prog. Org. Coat.* **1985**, *13*, 123–150.
(12) Arsu, N.; Aydin, M.; Yagci, Y.; Jockusch, S.; Turro, N. J. In *Photochemistry and UV Curing: New Trends*; Fouassier, J. P., Ed.; Research Signpost, Fort P.O.: Trivandrum, 2006; p 37/661.
(13) Yagci, Y.; Jockusch, S.; Turro, N. J. *Macromolecules* **2010**, *43*, 6245–6260.
(14) Olaj, O. F.; Bitai, I.; Hinkelmann, F. *Makromol. Chem.* **1987**, *188*, 1689–1702.
(15) Buback, M.; Gilbert, R. G.; Hutchinson, R. A.; Klumperman, B.; Kuchta, F.-D.; Manders, B. G.; O'Driscoll, K. F.; Russell, G. T.; Schweer, J. *Macromol. Chem. Phys.* **1995**, *196*, 3267–3280.
(16) Beuermann, S.; Buback, M.; Davis, T. P.; Gilbert, R. G.; Hutchinson, R. A.; Olaj, O. F.; Russell, G. T.; Schweer, J.; van Herk, A. M. *Macromol. Chem. Phys.* **1997**, *198*, 1545–1560.
(17) Beuermann, S.; Buback, M.; Davis, T. P.; Gilbert, R. G.; Hutchinson, R. A.; Kajiwara, A.; Klumperman, B.; Russell, G. T. *Macromol. Chem. Phys.* **2000**, *201*, 1355–1364.
(18) Beuermann, S.; Buback, M.; Davis, T. P.; García, N.; Gilbert, R. G.; Hutchinson, R. A.; Kajiwara, A.; Kamachi, M.; Lacík, I.; Russell, G. T. *Macromol. Chem. Phys.* **2003**, *204*, 1338–1350.
(19) Asua, J. M.; Beuermann, S.; Buback, M.; Castignolles, P.; Charleux, B.; Gilbert, R. G.; Hutchinson, R. A.; Leiza, J. R.; Nikitin, A. N.; Vairon, J.-P.; van Herk, A. M. *Macromol. Chem. Phys.* **2004**, *205*, 2151–2160.
(20) Beuermann, S.; Buback, M. *Prog. Polym. Sci.* **2002**, *27*, 191–254.
(21) Gruendling, T.; Voll, D.; Guilhaus, M.; Barner-Kowollik, C. *Macromol. Chem. Phys.* **2010**, *211*, 80–90.
(22) Aaserud, D. J.; Prokai, L.; Simonsick, J. W. J. *Anal. Chem.* **1999**, *71*, 4793–4799.
(23) Gruendling, T.; Guilhaus, M.; Barner-Kowollik, C. *Anal. Chem.* **2008**, *80*, 6915–6927.
(24) Gruendling, T.; Guilhaus, M.; Barner-Kowollik, C. *Macromolecules* **2009**, *42*, 6366–6374.
(25) Barner-Kowollik, C.; Günzler, F.; Junkers, T. *Macromolecules* **2008**, *41*, 8971–8973.
(26) Junkers, T.; Voll, D.; Barner-Kowollik, C. *e-Polym.* **2009**, 076.
(27) Barner-Kowollik, C.; Bennet, F.; Schneider-Baumann, M.; Voll, D.; Rölle, T.; Facke, T.; Weiser, M.-S.; Bruder, F.-K.; Junkers, T. *Polym. Chem.* **2010**, *1*, 470–479.
(28) Szablan, Z.; Lovestead, T. M.; Davis, T. P.; Stenzel, M. H.; Barner-Kowollik, C. *Macromolecules* **2006**, *40*, 26–39.
(29) Szablan, Z.; Junkers, T.; Koo, S. P. S.; Lovestead, T. M.; Davis, T. P.; Stenzel, M. H.; Barner-Kowollik, C. *Macromolecules* **2007**, *40*, 6820–6833.
(30) Vana, P.; Davis, T. P.; Barner-Kowollik, C. *Aust. J. Chem.* **2002**, *55*, 315–318.
(31) Günzler, F.; Wong, E. H. H.; Koo, S. P. S.; Junkers, T.; Barner-Kowollik, C. *Macromolecules* **2009**, *42*, 1488–1493.
(32) The term "(net) initiation efficiency" is employed to denote the propensity of a radical to commence macromolecular growth from the point of the laser pulse hitting the source molecule. It thus summarizes a true initiator efficiency (*net efficiency*), including all effects from the ability of the initiator to absorb light to the reactivity of the radical towards the monomer units.
(33) Spichty, M.; Turro, N. J.; Rist, G.; Birbaum, J.-L.; Dietliker, K.; Wolf, J.-P.; Gescheidt, G. *J. Photochem. Photobiol., A* **2001**, *142*, 209–213.
(34) Günzler, F. PhD Thesis, Göttingen, 2008.
(35) Buback, M.; Günzler, F.; Russell, G. T.; Vana, P. *Macromolecules* **2009**, *42*, 652–662.
(36) Weinstock, H. H.; Fuson, R. C. *J. Am. Chem. Soc.* **1936**, *58*, 1986–1988.
(37) Fuson, R. C.; Weinstock, H. H.; Ullyot, G. E. *J. Am. Chem. Soc.* **1935**, *57*, 1803–1804.
(38) Gray, A. R.; Fuson, R. C. *J. Am. Chem. Soc.* **1934**, *56*, 739–741.
(39) Gruendling, T.; Guilhaus, M.; Barner-Kowollik, C. *Macromol. Rapid Commun.* **2009**, *30*, 589–597.
(40) Weinstock, H. H.; Fuson, R. C. *J. Am. Chem. Soc.* **1936**, *58*, 1233–1236.
(41) Colley, C. S.; Grills, D. C.; Besley, N. A.; Jockusch, S.; Matousek, P.; Parker, A. W.; Towrie, M.; Turro, N. J.; Gill, P. M. W.; George, M. W. *J. Am. Chem. Soc.* **2002**, *124*, 14952–14958.